

# Evaluating the environmental quality impact of the 2008 Beijing Olympic Games: magnetic monitoring of street dust in Beijing Olympic Park

Qingqing Qiao,<sup>1</sup> Chunxia Zhang,<sup>1</sup> Baochun Huang<sup>1</sup> and John D. A. Piper<sup>2</sup>

<sup>1</sup>State Key Laboratory of Lithospheric Evolution, Institute of Geology and Geophysics, Chinese Academy of Sciences, Beijing 100029, China.

E-mail: qqqiao@mail.iggcas.ac.cn

<sup>2</sup>Geomagnetism Laboratory, Department of Earth and Ocean Sciences, University of Liverpool, Liverpool L69 7ZE, UK

Accepted 2011 August 17. Received 2011 August 16; in original form 2010 July 25

## SUMMARY

Aggressive traffic intervention and emission control measures implemented during the 2008 Olympic Games in Beijing created a valuable case study for evaluating the effectiveness of measures for mitigating environmental pollution and protecting public health. Results are reported here for a suite of magnetic and non-magnetic (microscopic, chemical and statistical) methods conducted on street dust deposits and parkland soils around the Olympic Park in Beijing. In both areas magnetic grains with multidomain properties predominate; grain sizes are coarser in the heavy traffic regions and finer in the park areas with evidence for particulate steel dust input in the former case. Traffic is the major source of anthropogenic magnetic particle-induced enhancement of magnetic susceptibility in street dust; however, domestic combustion processes (mainly coal burning) are found to contribute a significant magnetic signature in the urban environment during the winter. Due to the traffic intervention, magnetic compositions in street dust decreases significantly during the Olympic Games. Correlations between magnetic parameters and heavy metal contents prove that magnetic parameters can be used as proxies for heavy metal pollution.

**Key words** Environmental magnetism; Rock and mineral magnetism; Asia.

## 1 INTRODUCTION

Deposition and inhalation of atmospheric particulates are important contributions to environmental stress (Petrovský & Ellwood 1999). However, their effects can be transient and particulates that comprise street dust deposited and accumulated in the vicinity of roads only remain deposited at the site of fall for short periods (Adachi & Tainosho 2005; Tanner *et al.* 2008); they are readily washed away or resuspended back into the atmospheric aerosol by wind (Wise & Comrie 2005), or by movement of vehicles (Almeida *et al.* 2006). Similarly sourced particulates are also important contributors to house dust (Fergusson & Kim 1991; Adgate *et al.* 1998) and can degrade the quality of urban water runoff (Sartor & Gaboury 1984).

Street dust is omnipresent in the urban environment and human contact with it is inevitable and pervasive (Ng *et al.* 2003). Anthropogenic materials such as industrial and vehicle exhaust particles (Hunt *et al.* 1984; Flanders 1994), as well as natural biogenic materials such as leaves and other plant matter that can be pulverized by passing traffic (Rogge *et al.* 1993a), are direct contributors (Rogge *et al.* 1993b; Omar *et al.* 2007). Street dusts often contain elevated concentrations of a range of toxic elements (Banerjee 2003) and these have been reported to adversely affect human health and well-

being (Banerjee 2003; Harrison & Yin 2000). Hence it is important to gain a thorough understanding of the sources, characteristics and distributions of street dust and evaluate their impact on the atmospheric environment.

In urban areas anthropogenic particulates produced by combustion processes such as industrial, domestic and vehicle emissions (Hunt *et al.* 1984; Flanders 1994; Matzka & Maher 1999; Muxworthy *et al.* 2001, 2002; Shiton *et al.* 2005; Kim *et al.* 2007; Maher *et al.* 2008) and the abrasion products from asphalt and vehicle brake systems (Olson & Skogerboe 1975; Hoffmann *et al.* 1999; Chaparro *et al.* 2010) have significant magnetic properties. Among various anthropogenic particulates, iron-containing (and therefore paramagnetic or ferromagnetic) particulates commonly represent ~5–15 per cent of the total (Weber *et al.* 2000). Magnetite and less commonly hematite are ubiquitous in industrial fly-ashes and can display a wide range of grain sizes on a submicrometer to tens of micrometer scale (Petrovský & Ellwood 1999); the Verwey transition in magnetite tends to be weak and Curie points can vary from 565°C up to as high as 630°C, probably because disordered, non-stoichiometric structures are present and attributable to partially oxidized magnetite or maghemite (Dekkers & Pietersen 1992; Petrovský *et al.* 1998). The reception of such particulates by dust, soils, vegetation and sediments can result in abnormally high

magnetic loadings (Petrovský & Ellwood 1999; Hanesch *et al.* 2003). These magnetic particulates also often correlate with heavy metal concentrations (Beckwith *et al.* 1986; Charlesworth & Lees 1997; Gautam *et al.* 2005; Kim *et al.* 2007; Ng *et al.* 2003; Yang *et al.* 2010a) and organic compounds (Xie *et al.* 1999, 2000, 2001; Shiton *et al.* 2005), and these associations can be used to identify heavy metal and organic compound sources. Hence magnetic measurements can provide simple, rapid and non-destructive proxies for heavy metal pollution from aerosols. Furthermore, Morris *et al.* (1995) observe a significant correlation between mutagenicity and magnetic susceptibility in respirable urban airborne particulate matter, and these authors suggest that rapid magnetic susceptibility measurements can be used to pre-select filters for more extensive evaluation of biologic assays and the analysis of organic compounds.

Environmental magnetic methods based on the study of variations in mineral magnetic parameters have been successfully used for several decades to characterize and quantify degrees of pollution of air, water, vegetation and land systems (Petrovský & Ellwood 1999). Specific magnetic properties are also sensitive to grain-size variations (Dekkers 1997). Compared with traditional chemical methods, environmental magnetism provides a compositional tool, which is rapid, often grain-size indicative, non-destructive and inexpensive. It can also be sensitive to low detection levels and has now been widely shown to be an effective approach for studying urban pollution (Thompson & Oldfield 1986; Dekkers 1997; Hoffmann *et al.* 1999; Maher & Thompson 1999; Matzka & Maher 1999; Muxworthy *et al.* 2001; Spassov *et al.* 2004; Gautam *et al.* 2005; Shiton *et al.* 2005; Zhang *et al.* 2008). These investigations are complemented by the specific studies of Kim *et al.* (2007, 2008, 2009) and Yang *et al.* (2010a), which demonstrate that magnetic investigation of street dust is well suited to spatial and temporal pollution monitoring in urban areas.

The 29th Olympic and Para-Olympic Games were held between 2008 August 8 and September 17, in Beijing. As a densely populated city with more than 16 million residents and 3 million motor vehicles, traffic congestion and air pollution were two major challenges for the organizers of these games. Cities holding mega-events such as the Olympic Games usually try to achieve good air quality and traffic conditions by means of strategies such as temporary vehicular controls (Friedman *et al.* 2001; Lee *et al.* 2005; Frantzeskakis & Frantzeskakis 2006). Following this example, the City of Beijing implemented a series of air pollution control measures before and during the Olympic Games. These included the relocation of industrial plants with large emissions outside of the city and the implementation of new standards to reduce vehicular emission; the latter included limiting vehicle access during the event from 2008 July 20 to 2008 September 20 (Li *et al.* 2010b; Zhou *et al.* 2010). The experience gained demonstrated that temporary traffic management strategies could successfully improve urban traffic conditions and enhance air quality. The present project has aimed to gain an understanding of the impact of these measures using a holistic approach combining rock magnetic and geochemical methods. This paper reports an investigation of the spatial and temporal variations in the magnetic properties of street dust around this park before and during the Games. The magnetic investigation has been complemented by study of the microstructures of magnetic minerals extracts from the street dust and topsoil, and by heavy metal analyses. Although our sampling has been limited by temporal and spatial constraints on a premier national location, the collective data allow us to resolve some key temporal variations in anthropogenic magnetic particles from street dust and identify their sources.

## 2 MATERIAL AND METHODS

### 2.1 Study area and sampling strategy

The Chinese capital Beijing (39°54'N, 116°24'E) is located at the northern tip of the roughly triangular North China Plain. As one of four municipalities in China, the city spans some 16 800 km<sup>2</sup>; it is surrounded by the Yanshan and Taihang Mountains to the north and west while the southeast is open toward the lower reaches of the Gulf of Bohai. The Olympic Park is located at the northern end of the centre axis of Beijing and, as shown in Fig. 1, is bounded by the Qing River and the North 5th Ring Road network to the north with the latter taking a heavy traffic load (~300 000 vehicles day<sup>-1</sup>). The park is bounded by the comparably busy North 4th Ring Road to the south, the Anli Road to the east, and the Lincui Road to the west. The national stadium, swimming centre, gymnasium and Aquatic Park are all sited near to the Olympic Park.

To examine spatial and temporal variations of magnetic properties of dust, 24 sampling sites were selected: twenty-one street dust sampling sites were distributed along roads with different traffic densities or pavements around the Olympic Park, and three topsoil sampling sites were selected from the forest park inside the North 5th Ring Road (Fig. 1). The samples were collected bimonthly over a 12-month span between 2007 November and 2008 October using a nylon brush and non-magnetic scoop from squares 0.5 to 1 m<sup>2</sup> in area, and were transferred to clean, self-sealing polyethylene bags. Months during which sampling could not be undertaken were January, March, June, and August 2008; the causes for this were holidays, bad weather or final completion of venues for the Olympic Games and the associated aggressive traffic intervention. During July and September 2008 the forest park was completely closed to the public and eight street dust and six top soil samples could not be obtained during these 2 months. Each sampling campaign was carried out over a 7-day dry weather period following rainfall events. This approach is particularly important during the summer (rainy) season to ensure a sufficient quantity of recent dust samples and minimize any wash-out effects or redistribution by wind (*cf.* Matzka & Maher 1999). In total 178 dust samples recording 8 months of environmental impact were obtained from the 24 sites shown in Fig. 1. Following removal of any obvious artefacts such as cigarette debris, the samples were air-dried in the laboratory and sieved through a stainless steel sieve of size 500 μm. This procedure removes coarse-grained particles such as glass, plant debris, refuse and small stones. The samples were then compacted into standard 2 cm × 2 cm × 2 cm plastic sample cubes for magnetic measurements. A total of 356 cubes from 24 sites were prepared for analysis in this way.

### 2.2 Experimental methods

A dual frequency (470 and 4700 Hz) magnetic susceptibility meter (Bartington MS2) was used for susceptibility measurements on 2–7 g samples with values expressed as mass-specific susceptibilities  $\chi_{lf}$  and  $\chi_{hf}$ , respectively and a frequency-dependent susceptibility parameter determined from  $\chi_{fd}$  per cent =  $(\chi_{lf} - \chi_{hf})/\chi_{lf} \times 100$  per cent (Dearing *et al.* 1996). An hysteretic remanent magnetization (ARM) was imparted in a peak alternating field (AF) of 80 mT with a superimposed direct current (DC) bias field of 0.05 mT parallel to the AF. Isothermal remanent magnetization (IRM) determinations were performed with a Model 670 IRM Pulse Magnetizer and magnetic remanence was measured using a 2G-760 U-channel

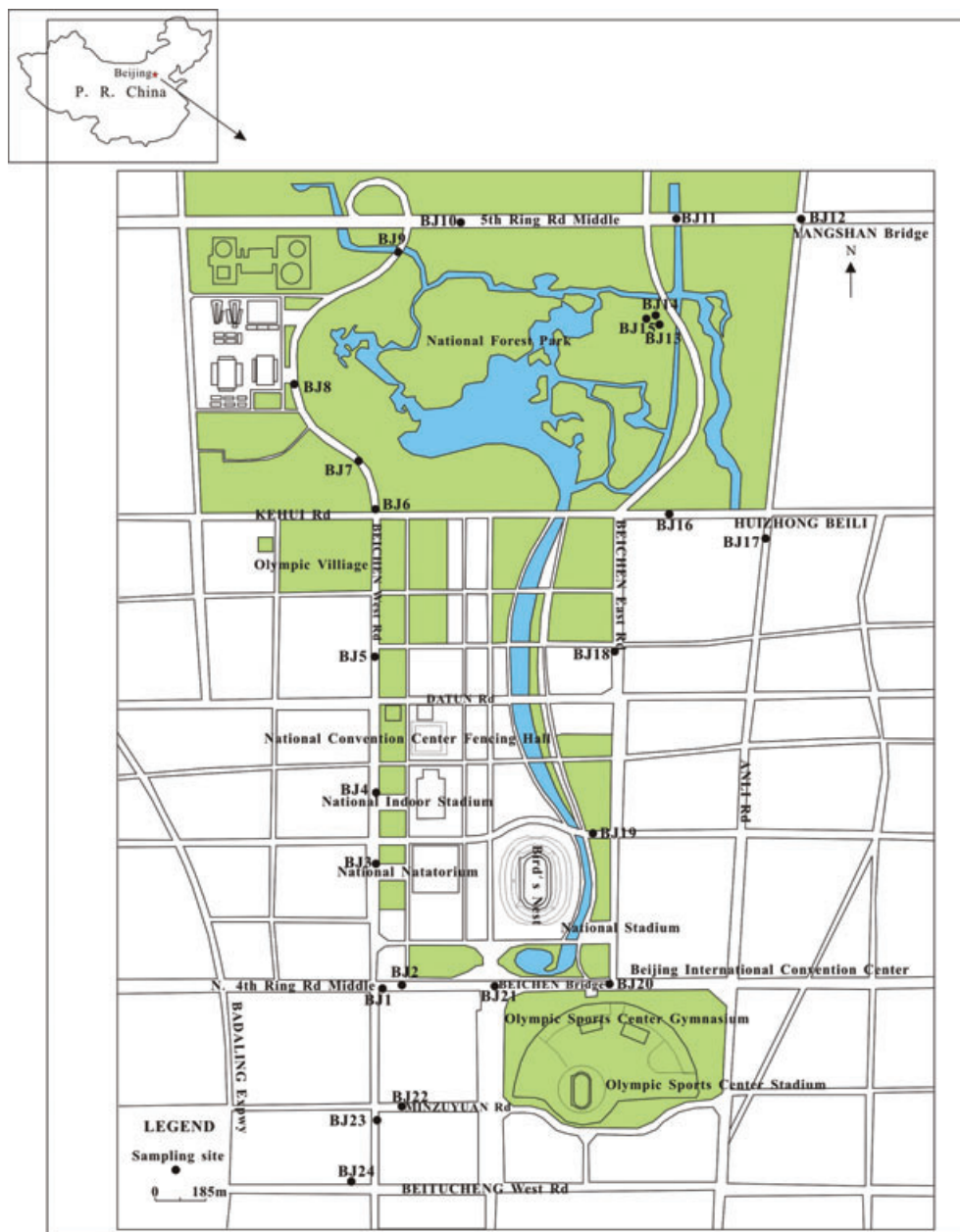


Figure 1. Sketch map showing the distribution of the 24 sampling locations (dots) in the area surrounding the Olympic Park, Beijing.

system. The IRM acquired in a field of 1.0 T was taken as the saturation IRM (SIRM) for this experiment. Temperature dependence of magnetic susceptibility for representative samples ( $\sim 200$  mg) between room temperature and  $700^{\circ}\text{C}$  was measured using an AGICO KLY-3 Kappabridge equipped with a CS-3 high-temperature furnace in an argon atmosphere with a measurement interval of  $2^{\circ}\text{C}$  at a heating and cooling rate of about  $9^{\circ}\text{C min}^{-1}$ ; Sampling sites were selected and categorized into traffic areas (2 sites) and the park area (1 site) with a total of 22 samples being measured. Magnetic hysteresis loops for representative samples were determined using a variable field translation balance (VFTB, Petersen Instruments) and values of saturation magnetization ( $M_s$ ), saturation remanence ( $M_{rs}$ ) and coercivity ( $B_c$ ) measured from the hysteresis loop following a paramagnetic slope correction; values of remanence coercivity ( $B_{cr}$ ) were obtained from the back-field demagnetization.

To determine characteristics of the magnetic materials such as grain size and shape, scanning electron microscopy (SEM) observations were carried out on particles separated from samples by hand magnet and sealed in a polyethylene bag. Compositions were determined by Energy Dispersive X-ray spectrometry (EDX) analysis using a LEO 1450VP equipped with INCA system (Oxford Instruments). The resolution factor was  $3.5\text{ nm}/30\text{ kV}$  (tungsten filament) and magnifications ranged from 9 to 90 000 at vacuum pressures from 1.0 to 400 Pa.

For analysis of the total concentration of heavy metals (Be, V, Cr, Co, Ni, Cu, Zn, Rb, Mo, Cd, Cs, Ba, Nd, Pb and Fe), dust samples were subjected to microwave digestion using  $\text{HNO}_3\text{--H}_2\text{O}_2\text{--HF}$ . Following complete digestion, the extracts were diluted to 50 mL and analysed by inductively coupled plasma-mass spectrometry (ICP-MS) employing the DZ/T0223–2001 method with HR-ICP-MS

(Element I) Finning MAT equipment in the Analytical Laboratory of the Beijing Research Institute of Uranium Geology. Pearson's correlation coefficient analysis was performed using a commercial statistics software package SPSS version 18.0 for Windows; spatial distributions of magnetic parameters were determined using contour maps produced by Surfer software.

### 3 RESULTS

#### 3.1 Spatial and temporal variations of magnetic parameters

$\chi$  and SIRM values for the 24 sampling sites collected in 2008 February reveal distinct spatial differences in magnetic mineral concentrations (Fig. 2). Samples from site BJ10 (on the ring road network taking heavy traffic) show the highest  $\chi$  value ( $378.26 \times 10^{-8} \text{ m}^3 \text{ kg}^{-1}$ ), whereas those from site BJ13 (park area) have the lowest value ( $23.98 \times 10^{-8} \text{ m}^3 \text{ kg}^{-1}$ , Fig. 2a). SIRM exhibits a spatial distribution pattern comparable to  $\chi$  (Fig. 2b) and further indicates that ferrimagnetic minerals (*sensu lato*) are the predominant magnetic carriers in these samples (Oldfield 1991; Verosub & Roberts 1995).

Temporal variations in magnetic concentration were traced using the more easily measured parameter  $\chi$ . Fig. 3 shows contour plots of magnetic susceptibility for the 24 sampling sites in the surroundings of the Olympic Park successively during the construction period of the Olympic venues and facilities (2007 November, 2007 December, 2008 February, 2008 April, 2008 May), before the opening of the Olympic Games (2008 July), during the Olympics (2008 September) and after the Olympics (2008 October). During the construction period of the Olympic venues and facilities there was little traffic

on both Beichen West and East Roads while the 5th Ring Road was a heavy traffic spot and, as shown in Fig. 3, the  $\chi$  values from Beichen West and East Roads are lower than those from the 5th Ring Road (Figs 3a–e). Nevertheless, the  $\chi$  values on these two roads clearly increased in the following months during (2008 September) and after (2008 October, see Figs 3g and h) the Olympic Games. This was especially the case during 2008 September (Fig. 3g) when a higher level of  $\chi$  is recorded for sampling sites in both Beichen East and West Roads. These were the main traffic roads and parking lots during the Olympic period, while during the construction period the  $\chi$  values in the winter (especially in 2008 February although with the exception of 2007 December) are markedly higher than at other times (Figs 3a–e). These records confirm the close relationship between magnetic signal and intensive anthropogenic contamination.

The different sampling locations show contrasts in the pattern of temporal variation of magnetic susceptibility: thus temporal variations of  $\chi$  are similar for sampling sites BJ3 and BJ5 which are both situated in Beichen West Road (Figs 1 and 4) where they were evidently more sensitive to meteorological conditions. The value of  $\chi$  decreased abruptly in 2007 December apparently in response to a heavy snowfall, which occurred 12 days before sampling. Meanwhile, because of the operation of domestic heating systems in the winter,  $\chi$  increased in 2008 February and then decreased again in 2008 April. However, samples collected from locations BJ10, BJ11 and BJ12 exhibit significantly different temporal variations in magnetic susceptibility although these three sampling sites are all situated inside the 5th Ring Road (Figs 1 and 4). The value of  $\chi$  for location BJ10 is higher than at the other two sites due to the constant heavy traffic density. Similarly, the value of  $\chi$  for location BJ12 located under the Yangshan Overpass is also higher than BJ11 situated under another overpass but used only by pedestrians. In

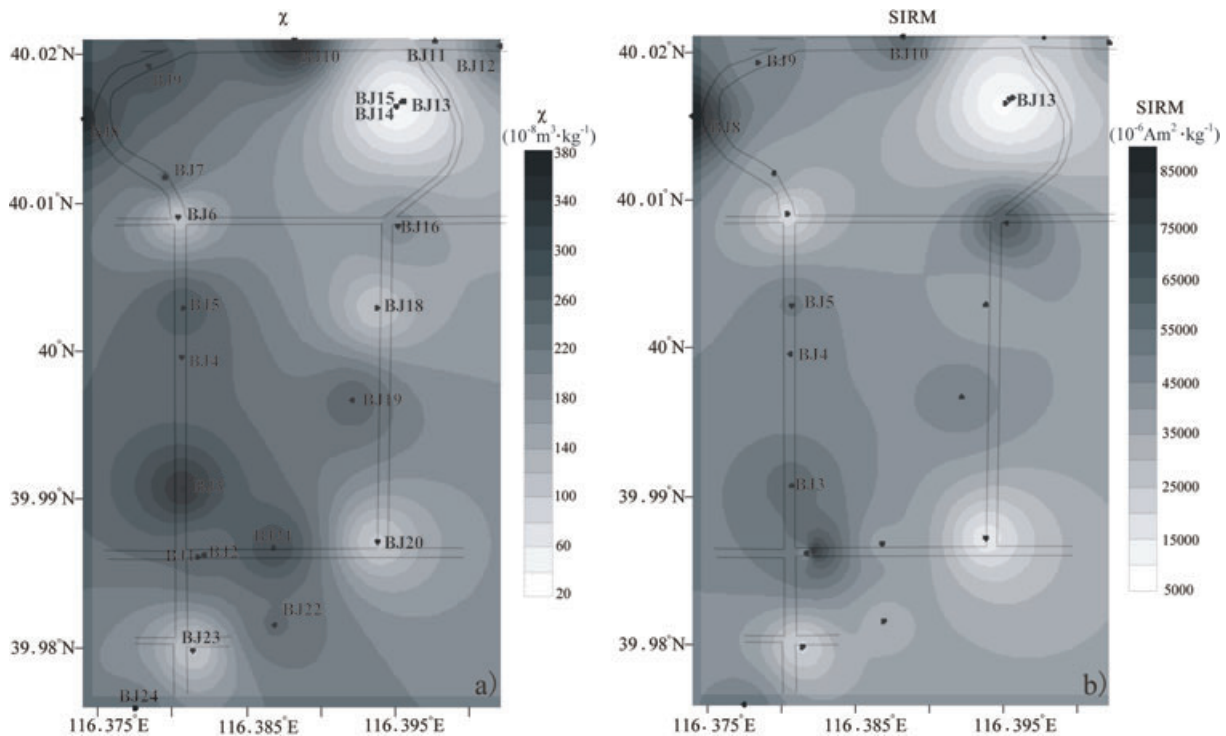


**Figure 2.** Contour maps of magnetic parameters for 2008 February in the Beijing Olympic Park, showing spatial distributions of magnetic concentration. Sampling locations are indicated by solid circles. (Owing to the shielding effect of buildings, GPS data could not be obtained for site BJ17 which is not shown here and in Figs 3 and 5.)

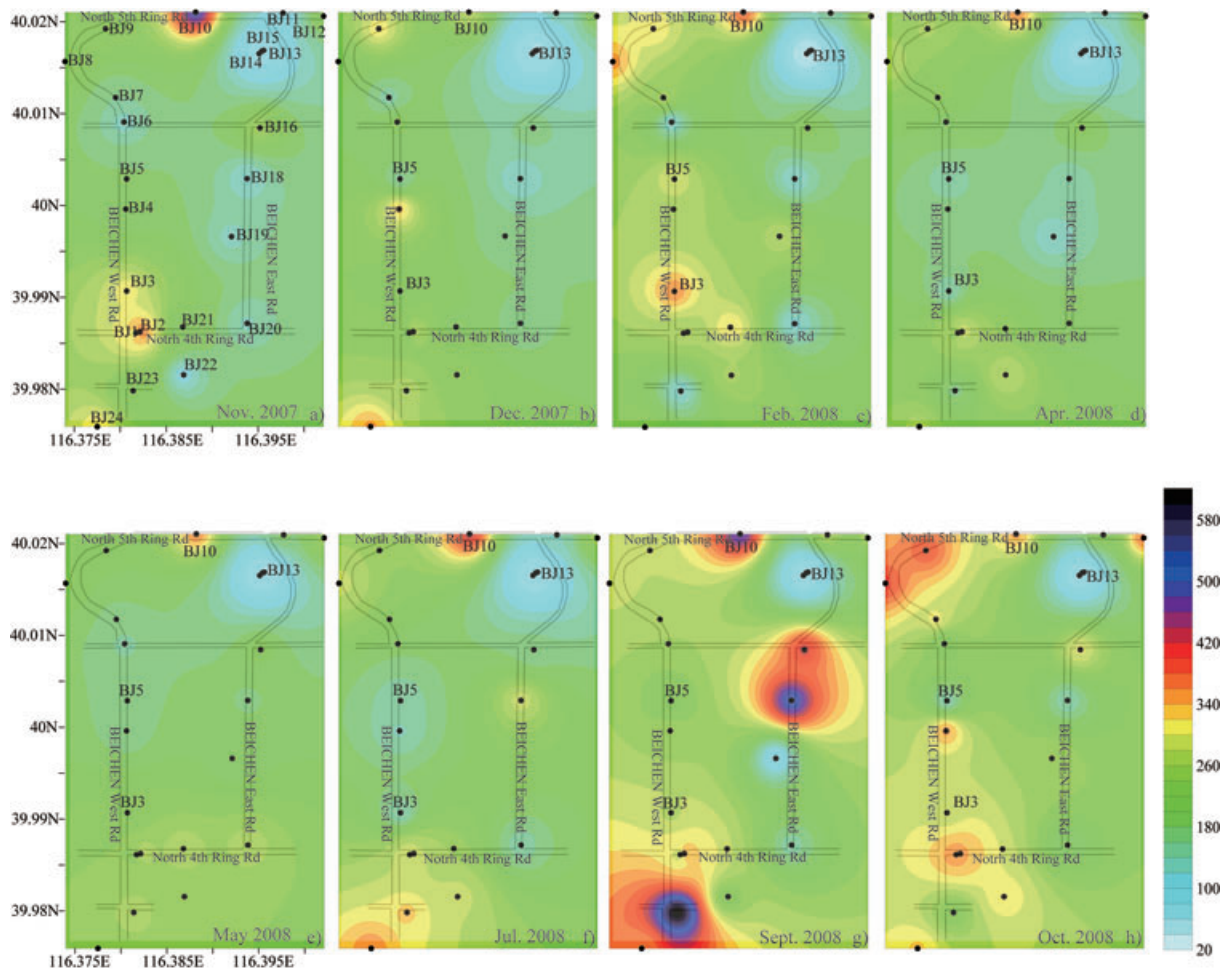


**Figure 3.** Contour plots of susceptibility for the 24 sampling sites in the area surrounding the Beijing Olympic Park during different months. The black dots represent the sampling locations. (a) 2007 November; (b) 2007 December; (c) 2008 February; (d) 2008 April; (e) 2008 May; (f) 2008 July; (g) 2008 September; (h) 2008 October.

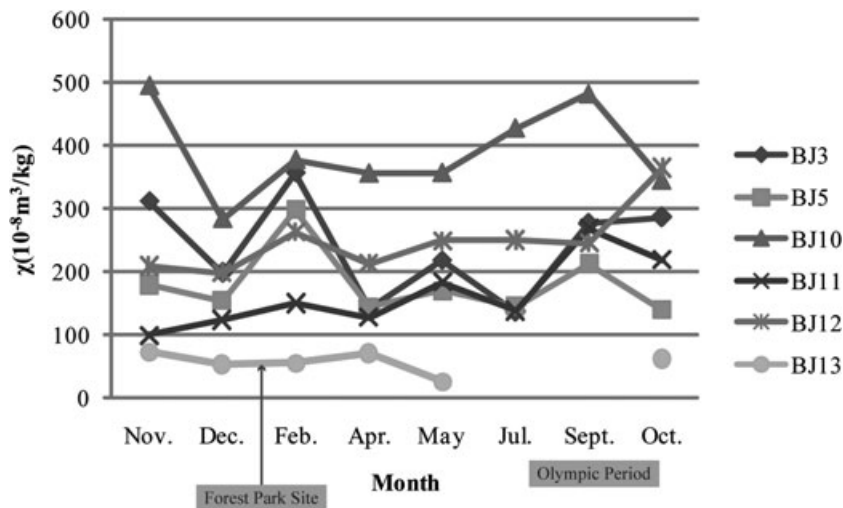


**Figure 4.** Diagrams showing seasonal variation of magnetic susceptibility at locations BJ3, BJ5 and locations BJ10–13. See Fig. 1 for sample locations.

contrast, samples from the forest park site BJ13, showed roughly constant and lower  $\chi$  values independent of sampling times (with the proviso that no samples were obtained during 2008 July and September due to aggressive traffic control measures).

Spatial variations of magnetic grain sizes in the dusts of 2008 February were determined using the ARM/ $\chi$  and ARM/SIRM ratios and results are summarized in Fig. 5. These ratios reveal a distinctive spatial pattern: in the vicinity of heavy traffic both lower

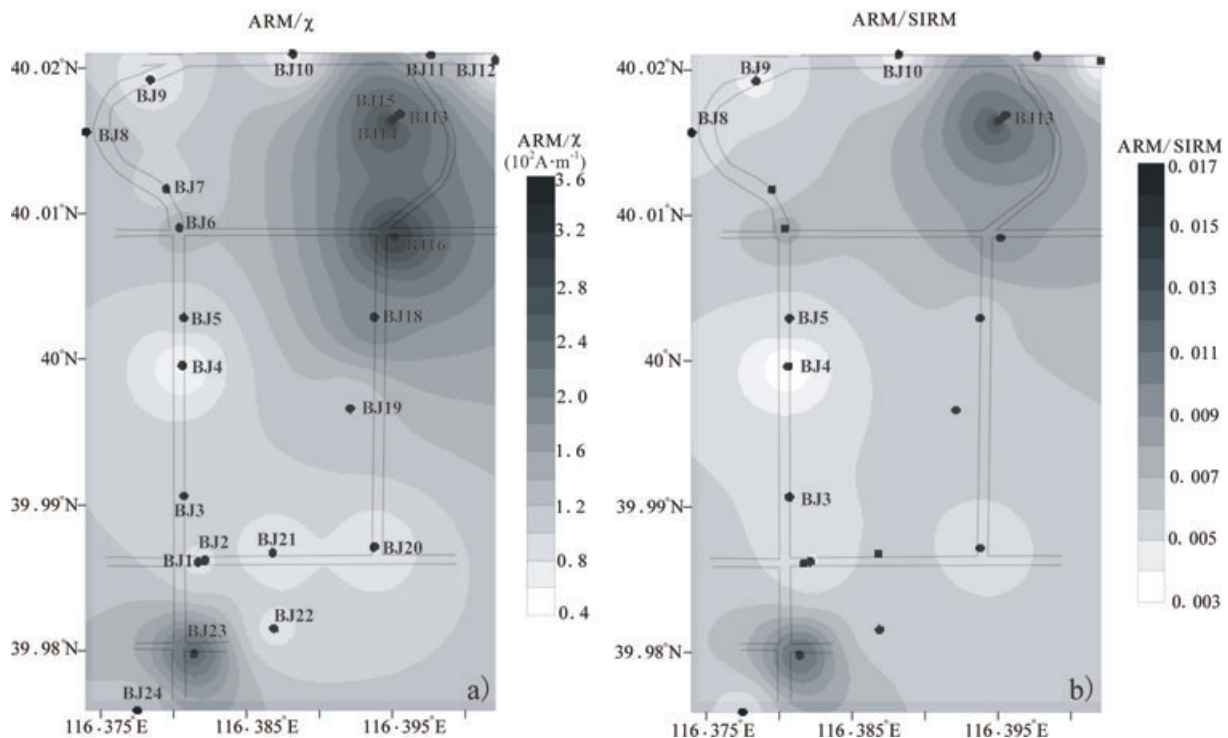


**Figure 5.** Contour maps of magnetic parameters for 2008 February in the Beijing Olympic Park, showing spatial distributions of grain size. Sampling locations are indicated by solid circles.

ARM/ $\chi$  and ARM/SIRM ratios suggest a predominance of coarse magnetic particles, whereas both higher ARM/ $\chi$  and ARM/SIRM ratios indicate higher proportions of fine particles in the samples from the forest park; this is comparable to results from studies reported elsewhere (*cf.* Maher 1988; Oldfield 1991; Yu *et al.* 1995; Hu *et al.* 2008) although our comparative sample from the roads is very limited. This contrast is further confirmed by a King plot of anhysteretic susceptibility ( $\chi_{ARM}$ ) against low-field susceptibility ( $\chi_{lf}$ ) (King *et al.* 1982; Evans & Heller 2003): samples from the park areas show relatively higher  $\chi_{ARM}/\chi_{lf}$  slope which implies the presence of finer-grained particles; in contrast the lower  $\chi_{ARM}/\chi_{lf}$  slopes from high and low traffic areas indicate coarser magnetic grain sizes (Fig. 6).

Temporal variations of the magnetic grain size in dusts can be evaluated using the Day-plot (Dunlop 2002), which shows a distinctive temporal pattern for samples collected from location BJ13 (topsoil from the forest park, Fig. 7). The grains sizes are coarser in the winter and finer during other seasons, indicating that the mean grain size of magnetic materials increases in winter. This trend is not however, obvious at location BJ6, BJ10 and BJ11 (street dust from the intersection of Beichen West Road and Kehui Road, the 5th Ring Road and the road under the overpass, respectively, Fig. 7), where the concentration of MD in the SD+MD mixture remained relatively stable compared to that at location BJ13; this evidence identifies no significant temporal changes in magnetic grain size in traffic areas.

All room temperature magnetic measurements indicate that magnetic mineralogy is dominated by coarse magnetic particles in the heavy traffic regions and fine particles in the park areas. The ferromagnet components in street dust decrease significantly during Olympic Games and after heavy snowfall, and increase in the winter.

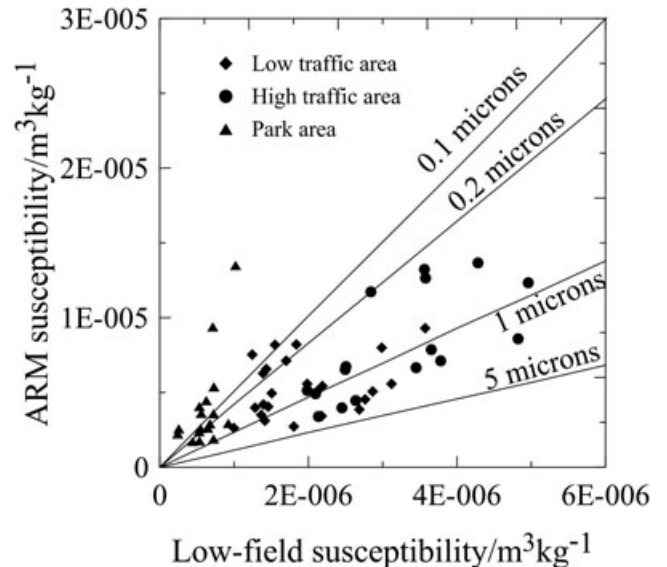


**Figure 6.** Bivariate plot of anhysteretic susceptibility ( $\chi_{ARM}$ ) versus low-field susceptibility ( $\chi_{lf}$ ) of the street dust and park samples following King *et al.* (1982). Note that samples from the park area contain finer grains than the low traffic and heavy traffic areas.

### 3.2 Magnetic mineralogy

The average magnetic parameters for topsoil and street dust are summarized in Table 1;  $\chi$  values of dusts from street and park areas contrast markedly at  $243.58$  and  $61.59 \times 10^{-8} \text{ m}^3 \text{ kg}^{-1}$ , respectively. SIRM and ARM of the street dust are both high.  $\chi_{fd}$  per cent is sensitive to the superparamagnetic (SP) component and if

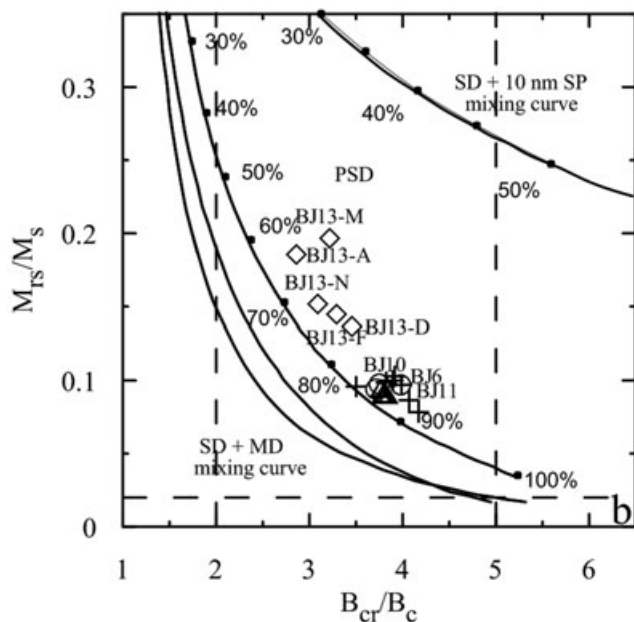


**Figure 7.** Day-plot for samples collected from the heavy traffic area (BJ6, circles; BJ10, triangles; BJ11, crosses) and the forest park (BJ13, diamonds). N–November 2007, D–December 2007, F–February 2008, A–April 2008, M–May 2008, O–October 2008. Domain boundaries and the SD+MD matrix line are from Dunlop (2002). Percentages in the plot represent the concentrations of MD in the SD+MD mixture.

$\chi_{fd}$  per cent > 4 per cent, the assemblage of magnetic grains contains a significant portion of SP particles; when  $\chi_{fd}$  per cent < 4 per cent the proportion of SP particles is likely to be low (Dearing *et al.* 1996). Thus magnetic carriers in the street dust yielding a mean  $\chi_{fd}$  per cent value of  $\sim 1.56$  per cent may be predominately coarse-grained particulates (Table 1). However, we qualify this conclusion by noting that the Bartington instrument senses larger SP particles within the 15 and 25 nm in size range. Dekkers & Pietersen (1992) measured a frequency dependence of 1–2 per cent when their TEM picture identified small nominally SP particles interacting magnetically; a minimal frequency dependence may not therefore necessarily be an unambiguous indicator of coarse material. The S-ratio ( $S = -IRM_{-300\text{mT}}/SIRM$ ) reflects the relative proportion of high-coercivity canted antiferromagnetic to low-coercivity ferrimagnetic minerals (Thompson & Oldfield 1986; Evans & Heller 2003) with high S-ratios (i.e. near 1.00) indicating that the ferrimagnetic fraction is dominant. To determine descriptive statistics for the S-ratio information properly, it is necessary to consider the ratio of the low and high coercivity components together. This can be performed

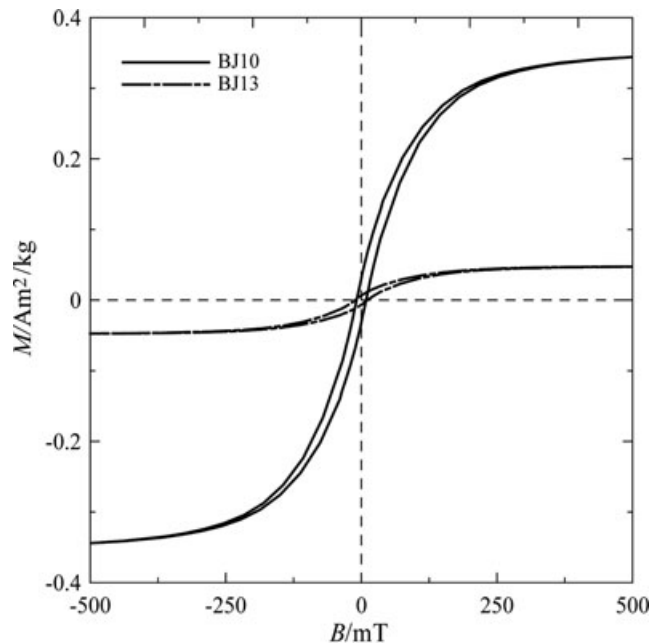


**Figure 8.** Hysteresis loops for representative samples collected from street dust location BJ10 and topsoil location BJ13. The illustrated plot shows the segment of the loops below 500 mT.

using the additive-log-ratio (alr) transform (Heslop 2009 and references therein) and yields 0.95 (street dust) and 0.90 (topsoil) as a measure of the ‘location’ of the data. The derived 95 per cent confidence limits are 0.94–0.96 for street dust and 0.88–0.92 for topsoil (Table 1). The mean S-ratios for topsoil and street dust also suggested that ferrimagnets predominate over antiferromagnets in these samples (Table 1).

The typical thin hysteresis loops shown in Fig. 8 approach magnetic saturation in fields of  $\sim 300$  mT and indicate that low-coercivity magnetite is the dominant ferromagnet. Magnetic minerals in street dust and topsoil can be identified by temperature-dependent susceptibility ( $\chi$ – $T$ ) cycles. Fig. 9 illustrates  $\chi$ – $T$  curves for representative dust samples from the park (BJ13) and traffic (BJ10) areas during 2007 November, 2008 February and 2008 May, respectively performed in an argon atmosphere. The increased susceptibility below 250°C and the peaks around 250–300°C may indicate ultrafine particles reaching the SD to SP transition at these temperatures (Oches & Banerjee 1996; Deng *et al.* 2004; Liu *et al.* 2005). The susceptibility increases sharply to just below the Curie temperature of magnetite, and shows a  $T_c$  of  $\sim 580^\circ\text{C}$  which identifies magnetite as the major contributor to  $\chi$ .

**Table 1.** Summary of the magnetic parameters of topsoil and street dust in Beijing Olympic Park.

|  |                               | Topsoil ( $n = 18$ ) | Street dust ( $n = 160$ ) |
|--|-------------------------------|----------------------|---------------------------|
| $\chi$ ( $10^{-8} \text{ m}^3 \text{ kg}^{-1}$ ) | Range                         | 23.98–102.25         | 84.48–618.81              |
|  | Mean $\pm$ SD                 | $61.59 \pm 4.58$     | $243.58 \pm 92.84$        |
| SIRM ( $10^{-5} \text{ Am}^2 \text{ kg}^{-1}$ )  | Range                         | 530.61–4350.39       | 1260.31–32233.87          |
|  | Mean $\pm$ SD                 | $1492.38 \pm 200.99$ | $5324.85 \pm 3801.83$     |
| ARM ( $10^{-6} \text{ Am}^2 \text{ kg}^{-1}$ )   | Range                         | 68.44–537.37         | 84.45–1534.18             |
|  | Mean $\pm$ SD                 | $158.41 \pm 29.57$   | $267.21 \pm 159.35$       |
| $\chi_{fd}$ per cent                             | Range                         | 0.00–7.41            | 0.00–12.20                |
|  | Mean $\pm$ SD                 | $2.95 \pm 0.40$      | $1.56 \pm 1.29$           |
|  | 95 per cent confidence limits | 0.88–0.92            | 0.94–0.96                 |
| S-ratio  | Mean                          | $0.90 \pm 0.01$      | $0.95 \pm 0.05$           |

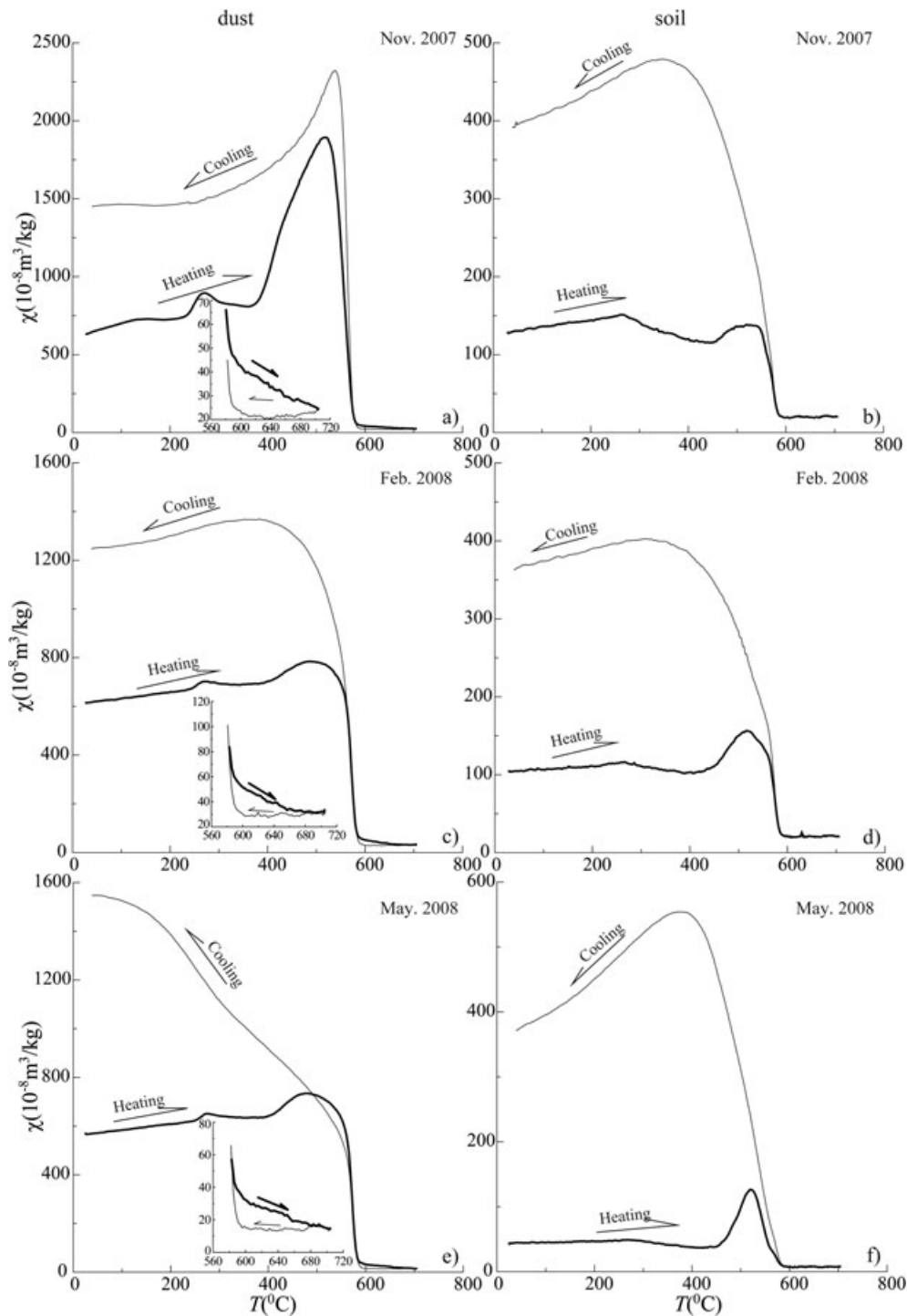


**Figure 9.** Thermomagnetic curves (temperature versus magnetic susceptibility) for representative samples collected from a heavy traffic area (BJ10, examples a, c and e) and the forest park (BJ13, examples b, d and f) in 2007 November, 2008 February and 2008 May, respectively. Heating and cooling curves are indicated by thick and fine lines, respectively.

All samples are irreversible with cooling paths above heating trajectories. A primary prevalent contribution of magnetite is therefore evident with production of new magnetite during the heating process (Jordanova *et al.* 2004; Petrovský & Kapička 2006; Kim *et al.* 2009).

The very different maximum susceptibility values associated with contrasting  $\chi$ - $T$  behaviours at higher temperatures of 600–700 °C

identify distinct differences between topsoil and street dust samples: in topsoil the cooling curve shapes are essentially reversible and there is no detectable contribution of hematite that might result for example, from wind-blown dust. In street dust however, the cooling curves above 600 °C are below the heating curves but then sharply increase at 580 °C (Figs 9a, c and e); this effect coupled with the decreasing tail in the heating curves above 600 °C could be due to

the transformation of iron sourced in particulate steel dust from engine wear and steel mills (Hopke *et al.* 1980; Zheng & Zhang 2008; Li *et al.* 2010a; Zhang *et al.* 2010). Thus, in summary, the mineral magnetic results (Table 1 and Figs 7–9) show that PSD-MD magnetite is the dominant ferrimagnetic phase in the street dust and topsoil samples.

### 3.3 Electron microscope analysis

SEM investigation can provide information on grain size and morphology of particles in the micrometer scale (Utsunomiya & Ewing 2003); examples showing size and morphologic characteristics of magnetic extracts are illustrated in Fig. 10. Magnetic

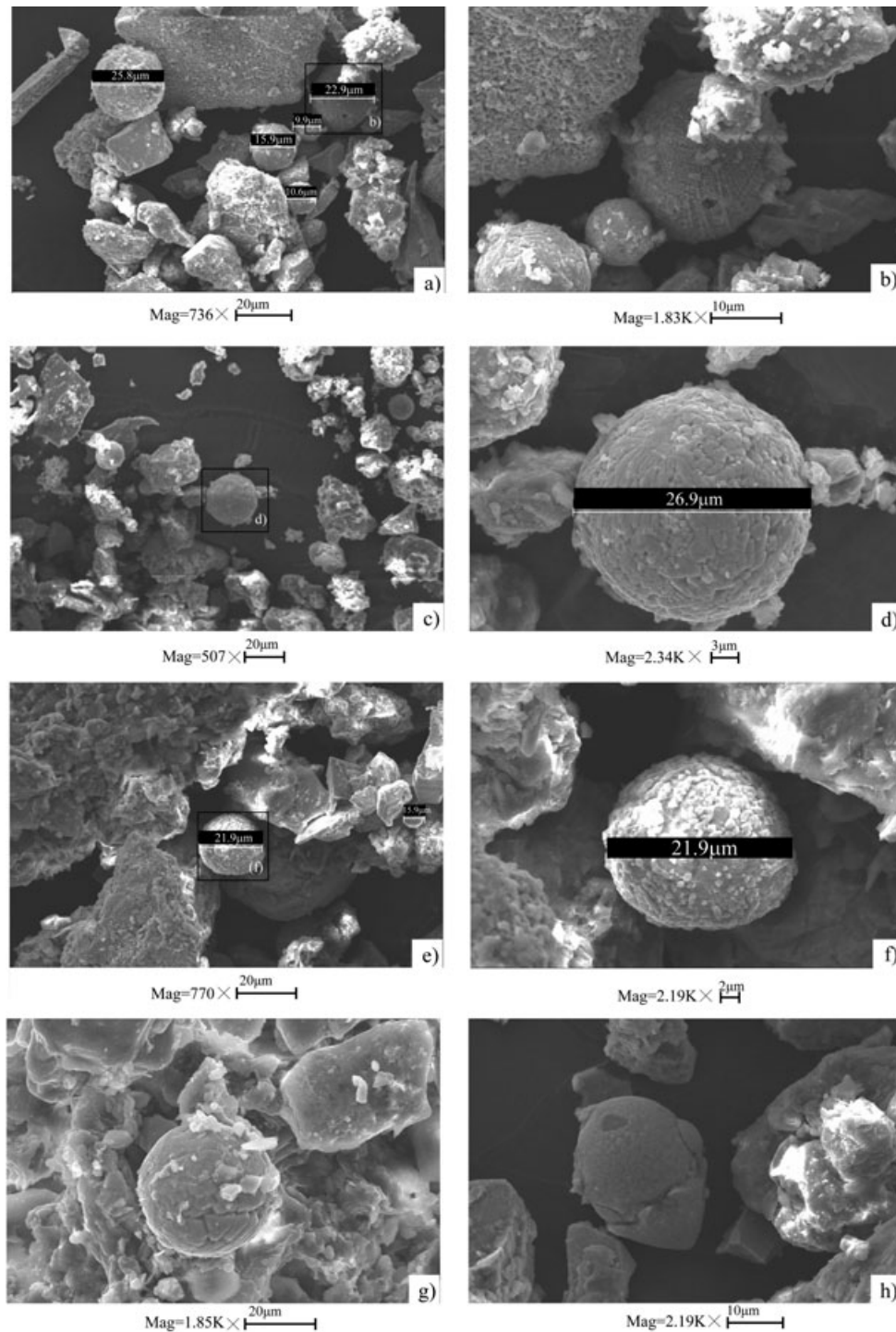


**Figure 10.** SEM images of magnetic extracts: (a) iron-oxides in the street dust from Site BJ10 in 2008 February during the period when domestic heating systems were operating; (b) a representative iron-oxide of the sample shown in (a) illustrating a coiled shape; (c) iron-oxides in the street dust from Site BJ10 in 2008 May (when domestic heating systems were not operating); (d) a representative iron-oxide of example (c) showing an orange peel form; (e) iron-oxides in the topsoil from Site BJ13 during the winter period (2008 February); (f) a representative iron-oxide of example (e) showing arborization; (g) a typical example of a football-shaped iron-oxide spherule; (h) iron-oxides in the topsoil from Site BJ13 during the spring-summer period (2008 May) for seasonal comparison with (e).

particulates of various morphologies were observed (Fig. 10) consisting of spherules and irregular aggregate shapes. EDX analysis also identifies magnetic spherules composed predominantly of Fe, O with additional minor element contributions including Al, S, Si and Ca. Grain-diameters of these spherical magnetic particulates range from 7 to 27  $\mu\text{m}$ . Figs 10(a) and (c) show representative SEM images of the magnetic particles in street dust samples during the winter and other seasons, respectively where the morphologies include large angular and spherical shapes; the spherule populations are higher in the winter than during other seasons. EDX analysis identifies these particles as mainly iron-oxides. Figs 10(b) and (d) show representative SEM images of rounded iron-oxides ranging from  $\sim 23$  to  $\sim 27$   $\mu\text{m}$  in diameter; these particles also tend to show coiling with orange peel morphologies. Most of the magnetic particles in the topsoil samples from the forest park are a mixture of irregular and spherular iron-oxides (Figs 10e and h) and these are typically smaller than iron-oxides in the street dust samples. Figs 10(f) and (g) show representative subrounded iron-oxides ( $\sim 22$   $\mu\text{m}$  in length) with the surfaces comparable to the 'arborized and football' forms described by Zhang *et al.* (2009). The spherical grains in Fig. 11(a) have high iron contents in addition to small

amounts of Al, S, Ca and Si, impurities found in the Gondwana coals used extensively for power generation and industrial purposes in China. In the angular grains however, only Fe is identified and these non-spherical Fe-rich particles have probably been released from vehicles via exhaust emissions from engines and from the abrasion or corrosion of vehicle body work (Olson & Skogerboe 1975; Hoffmann *et al.* 1999; Kim *et al.* 2007). We find that the element sulfur is found only in the spherical magnetic particulates from samples collected in winter, indicating an anthropogenic origin resulting from fossil fuel combustion. It is suggested that these spherules are produced during combustion from the melting of trace quantities of Fe in fossil fuels (Shiton *et al.* 2005) with the contents of other elements including Al and Ca dependent on the composition of the fuel (Moreno *et al.* 2003; Kim *et al.* 2009). Fig. 11(b) contrasts electron micrographs of topsoil particles for the winter period together with their EDX spectra. These spectra show dominant peaks of Fe, along with small peaks of Si in the spherical magnetic particulates. The angular grains in topsoil however, show a variety of chemical compositions not including Fe, and Fig. 11(b) highlights an angular grain, presumably quartz, composed of O and Si.

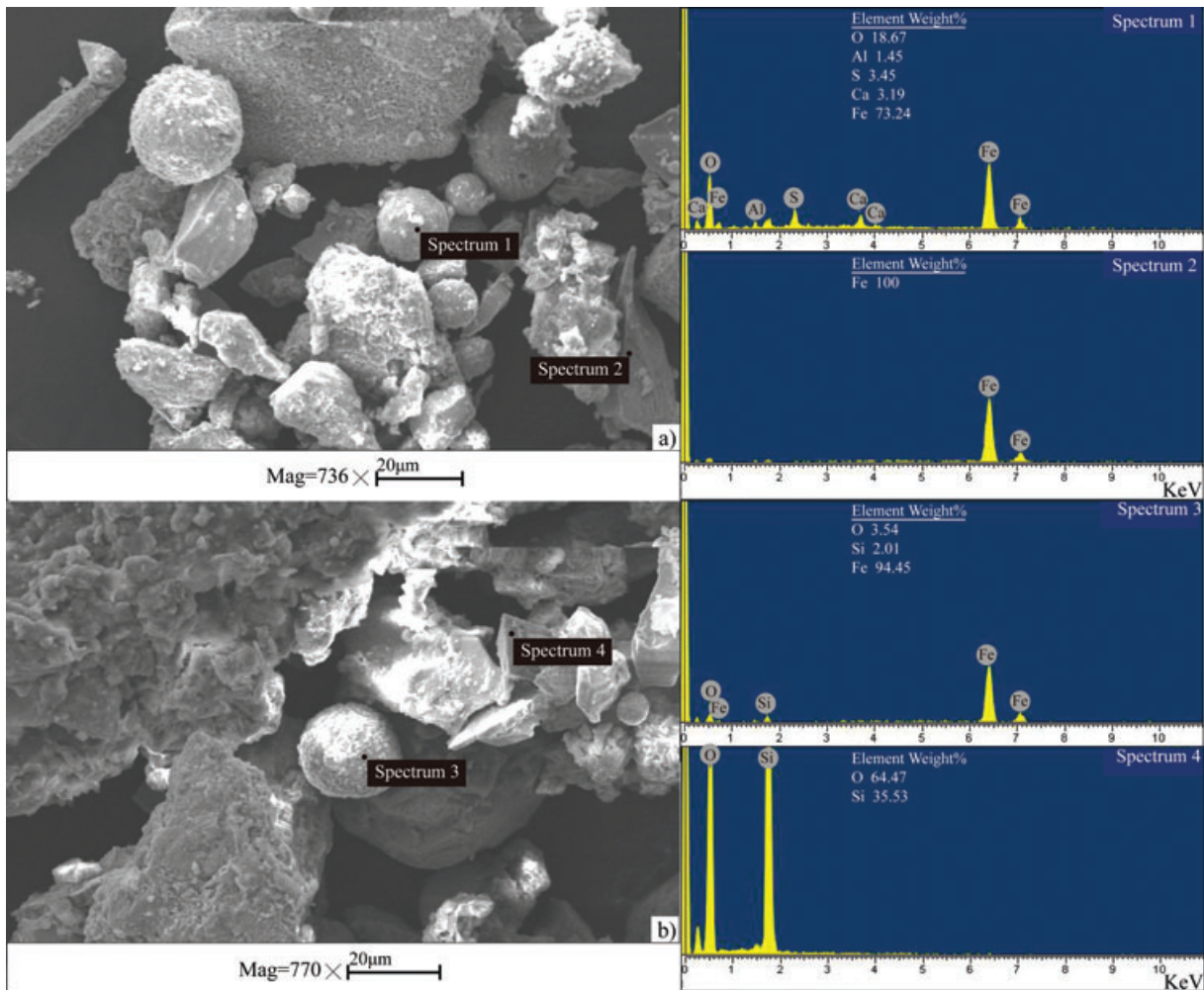


**Figure 11.** (a) EDX analyses for street dust samples from location BJ10 (street dust) during the winter (2008 February). Semi-quantitative elemental spectra shown for samples collected in 2008 February are Fe, O, Ca, Al and S. The presence of the element S in the winter sample is a signature of the contribution from coal burning; (b) EDX analyses for topsoil samples from location BJ13 (topsoil, forest park) during the winter (2008 February). The elements for samples collected in 2008 February are Fe, O and Si.

### 3.4 Heavy metals and their relationship to magnetic parameters

The concentrations of 14 elements (in  $\mu\text{g g}^{-1}$ ) are shown in Table 2 and a comparison of concentrations of Fe, Pb, Zn, Cu, Co and Ni is shown in Fig. 12 where the mean concentrations of these metals present in the BJ10 (street dust) segment are seen to be higher than those in BJ13 (topsoil, forest park), especially the concentration of Zn (Fig. 12c). To assess relative heavy metal toxicity and how much each sample exceeds the element concentrations for natural environments, we use the Tomlinson pollution load index (PLI, Angulo 1996). The PLI is defined as the  $n$ th root of the multiplication of the concentration factors  $CF_{HM}$ :  $(CF_{HM1}CF_{HM2}CF_{HM3}\dots\times CF_{HMn})^{1/n}$  where  $n$  is the number of metals and  $CF_{HM}$  is the contamination factor calculated from: Metal concentration in the material/Background value of the metal (Tomlinson *et al.* 1980); the lowest concentration value for each element was used as background value. This index is approximately unity if there is no significant pollution and can range up to values of  $\sim 2$  in environments with high metal toxicities (Yang *et al.* 2010a). Although this parameter is source-dependant to a degree, it appears to be an effective qualitative monitor of toxicity in this case: the PLI in the heavy traffic area of BJ10 ranges from 1.14 to 1.44 with a mean value of 1.22, and the PLI in the forest park at BJ13 ranges from 1.09 to 1.23 with a mean value of 1.17.

Table 3 lists Pearson's correlation coefficients between element concentrations and magnetic parameters. This table identifies a significant correlation between  $\chi$  and SIRM and each of the elements

Fe, V, Cr, Co, Ni, Cu, Zn, Pb and Cd. In contrast,  $\chi_{fd}$  correlates in a negative way with concentrations of all heavy metals (Table 3). ARM also correlates with these elements with the exception of V, Cu and Zn. The difference in the correlations between magnetic parameters and heavy metals is probably a reflection of intermixture of elements from a variety of sources and their association with different magnetic minerals (Yang *et al.* 2010a).

## 4 DISCUSSION

### 4.1 Sources of the magnetic materials

Collectively the high values of  $\chi$  and SIRM, the low ratios of ARM/ $\chi$  and ARM/SIRM, and the presence of coarse-grained magnetite as the primary magnetic carrier in heavy traffic regions (Figs 2, 3, 5 and 9) show that magnetic properties of street dust are dominated by ferrimagnetic minerals with an anthropogenic origin. This compares with the results of earlier studies such as those of Fialova *et al.* (2006). Photomicrographs of the magnetic extracts show mostly angular particles and spherules (Figs 10a and c); these are comparable to the magnetic spherules in fly ashes and roadside dust derived mainly from fossil fuel combustion and vehicles as documented by Matzka & Maher (1999) and Muxworthy *et al.* (2001). We attribute the angular particles to engine and brake abrasion, and the magnetic spherules to domestic and industrial combustion.

Sites BJ13, BJ14 and BJ15 (Fig. 1) are most representative of the natural background and provide a relative reference for measurement of anthropogenic input into the study area. Magnetic,

**Table 2.** Comparative heavy metal concentrations and PLI for road (BJ10) and park (BJ13) sites.

| Element<br>(concentration in $\mu\text{g g}^{-1}$ ) |               | BJ10 ( $n = 6$ )        | BJ13 ( $n = 6$ )       |
|---|---------------|-------------------------|------------------------|
| Fe  | Range         | 34361.00–40697.00       | 27442.00–31246.00      |
|   | Mean $\pm$ SD | 37273.17 $\pm$ 2347.51  | 29430.33 $\pm$ 1325.59 |
| V   | Range         | 90.40–108.00            | 81.90–89.10            |
|   | Mean $\pm$ SD | 98.00 $\pm$ 7.05        | 84.78 $\pm$ 2.77       |
| Cr  | Range         | 73.40–88.90             | 50.00–58.80            |
|   | Mean $\pm$ SD | 79.65 $\pm$ 6.01        | 54.90 $\pm$ 3.06       |
| Co  | Range         | 12.30–15.00             | 11.30–12.10            |
|   | Mean $\pm$ SD | 14.13 $\pm$ 0.98        | 11.73 $\pm$ 0.29       |
| Ni  | Range         | 31.30–43.80             | 22.10–27.50            |
|   | Mean $\pm$ SD | 36.67 $\pm$ 4.48        | 25.25 $\pm$ 1.82       |
| Cu  | Range         | 63.20–146.00            | 27.50–47.00            |
|   | Mean $\pm$ SD | 97.13 $\pm$ 32.27       | 36.02 $\pm$ 7.98       |
| Zn  | Range         | 15106.00–70828.00       | 72.10–134.00           |
|   | Mean $\pm$ SD | 32968.17 $\pm$ 19695.27 | 106.27 $\pm$ 24.10     |
| Pb  | Range         | 68.10–114.00            | 27.10–46.60            |
|   | Mean $\pm$ SD | 79.30 $\pm$ 17.26       | 38.70 $\pm$ 7.16       |
| Rb  | Range         | 43.20–74.40             | 81.90–95.60            |
|   | Mean $\pm$ SD | 62.43 $\pm$ 11.00       | 89.88 $\pm$ 4.86       |
| Sr  | Range         | 287.00–340.00           | 244.00–325.00          |
|   | Mean $\pm$ SD | 310.83 $\pm$ 20.05      | 271.33 $\pm$ 27.98     |
| Y   | Range         | 24.00–31.50             | 22.10–25.50            |
|   | Mean $\pm$ SD | 27.78 $\pm$ 3.12        | 24.22 $\pm$ 1.27       |
| Cd  | Range         | 0.55–0.81               | 0.17–0.35              |
|   | Mean $\pm$ SD | 0.66 $\pm$ 0.09         | 0.23 $\pm$ 0.07        |
| Ba  | Range         | 527.00–810.00           | 520.00–576.00          |
|   | Mean $\pm$ SD | 625.00 $\pm$ 97.62      | 544.83 $\pm$ 19.06     |
| Zr  | Range         | 142.00–181.00           | 119.00–176.00          |
|   | Mean $\pm$ SD | 163.17 $\pm$ 15.01      | 149.00 $\pm$ 20.33     |
| PLI   | Range         | 1.14–1.44               | 1.09–1.23              |
|   | Mean $\pm$ SD | 1.22 $\pm$ 0.11         | 1.17 $\pm$ 0.05        |

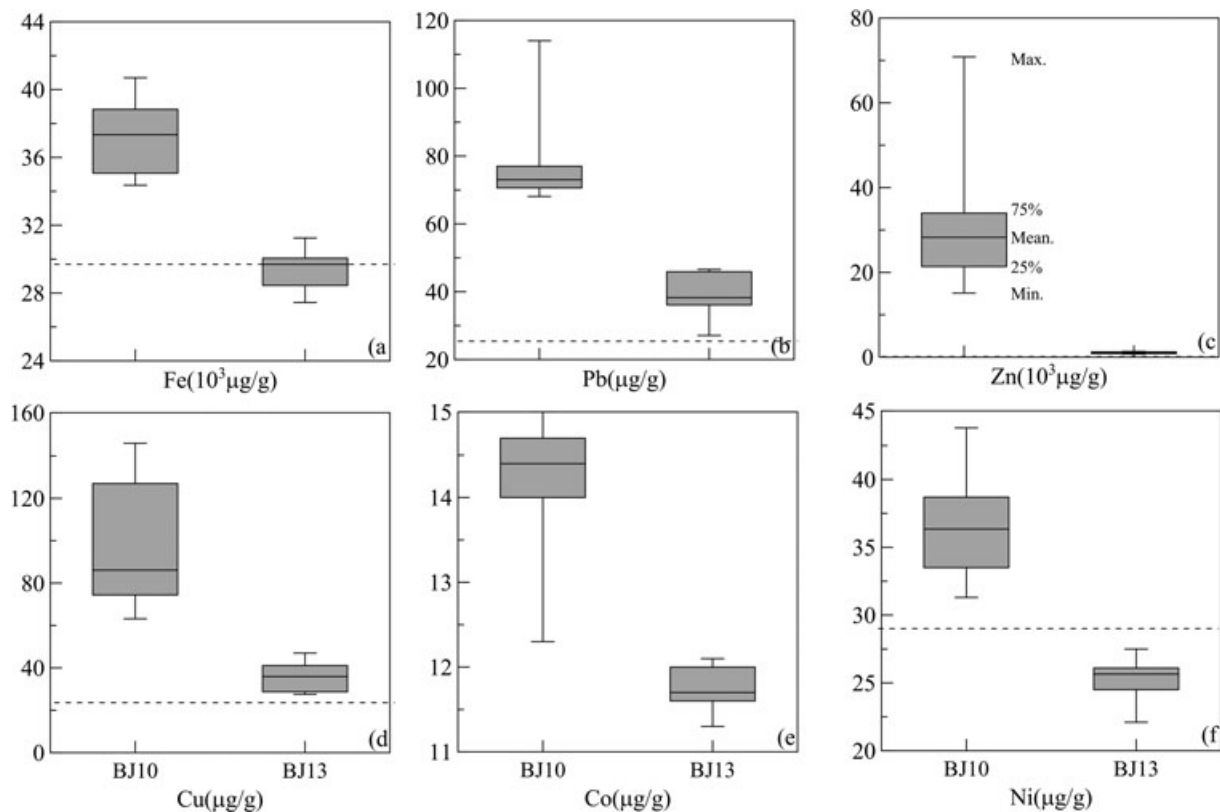


**Figure 12.** Comparison of heavy metal concentrations of street dust at sites BJ10 (street dust) and BJ13 (topsoil, forest park). The boxes in the box plot give the interquartile range of values; the lines in the boxes give the median values. The dashed lines show mean values of heavy metal concentrations in the soils of Beijing.

**Table 3.** Pearson correlation coefficient between selected heavy metal levels and magnetic parameters for street dust ( $n = 12$ ).

|             | Fe                 | V                  | Cr                 | Co                 | Ni                 | Cu                 | Zn                 | Pb                 | Cd                 |
|-------------|--------------------|--------------------|--------------------|--------------------|--------------------|--------------------|--------------------|--------------------|--------------------|
| $\chi$      | 0.967 <sup>a</sup> | 0.788 <sup>a</sup> | 0.967 <sup>a</sup> | 0.904 <sup>a</sup> | 0.954 <sup>a</sup> | 0.896 <sup>a</sup> | 0.908 <sup>a</sup> | 0.950 <sup>a</sup> | 0.869 <sup>a</sup> |
| SIRM        | 0.873 <sup>a</sup> | 0.705 <sup>b</sup> | 0.840 <sup>a</sup> | 0.878 <sup>a</sup> | 0.850 <sup>a</sup> | 0.660 <sup>b</sup> | 0.742 <sup>a</sup> | 0.818 <sup>a</sup> | 0.862 <sup>a</sup> |
| ARM         | 0.715 <sup>a</sup> | 0.551              | 0.642 <sup>b</sup> | 0.750 <sup>a</sup> | 0.699 <sup>b</sup> | 0.460              | 0.558              | 0.667 <sup>b</sup> | 0.693 <sup>b</sup> |
| $\chi_{fd}$ | -0.574             | -0.351             | -0.515             | -0.556             | -0.535             | -0.405             | -0.371             | -0.497             | -0.407             |

<sup>a</sup>Correlation is significant at the 0.01 level (2-tailed).

<sup>b</sup>Correlation is significant at the 0.05 level (2-tailed).

SEM and EDX results (Figs 2–7, 9–11) reveal that smaller magnetite occurring as spherules is the dominant ferrimagnetic phase with small amounts of SP magnetic particles in the topsoil. According to Maher (1998) ultrafine magnetic grains comprising primarily SP but also including SD grains, are produced mainly by fermentation and magnetotactic bacteria in soils; in contrast, coarse grains incorporating PSD and MD magnetic structures, are mainly the result of anthropogenic activities such as combustion and abrasion from vehicular activity (e.g. Flanders 1999; Kapička *et al.* 1999; Hoffmann *et al.* 1999). Anthropogenic dust input is characterized by higher magnetic concentrations (Fig. 9) residing in coarser ferrimagnetic grains (Figs 6 and 7) of spherical and angular shapes (Fig. 10).

The grain sizes of magnetic particles in street dust samples resulting from heavy traffic densities are concentrated in the range 80–90 per cent of the MD+PSD mixture curve regardless of what time of the year the samples are collected (Fig. 7). Since traffic

volumes vary little throughout the year, the magnetic particles in the street dust samples appear to be derived largely from vehicle abrasion and exhaust emission where they accumulate largely at the road edges (*cf.* Hoffmann *et al.* 1999; Knab *et al.* 2001; Zhang *et al.* 2006). In contrast, magnetic grain sizes in topsoil are dispersed within the range of 60–80 per cent of the mixture curve and show a temporal pattern: particles are coarser in winter than during other seasons. The presence of element S in samples (Fig. 11a) indicates that anthropogenic particulates released from fossil fuel combustion in domestic heating systems during the winter are evidently responsible (e.g. Flanders 1994).

Coal is an important energy source in Beijing as in other Northern China cities especially during the winter when domestic heating systems correlate with increasing magnetic susceptibilities (Fig. 3c). The official space-heating season is from November to March when coal consumption in Beijing is ~30 million tons (Feng *et al.* 2005). This signature was modulated in 2007 December when heavy

snowfall significantly decreased vehicle use and consequently magnetic susceptibility. Temporal variations of magnetic susceptibility from sampling locations BJ3 and BJ5 show variations in  $\chi$  reflecting magnetic mineral concentrations during the winter (Fig. 4) linked to release of magnetic spherules from fossil-fuel combustion. This effect is enhanced here because the aerosol is constrained: the city of Beijing is surrounded by mountains on three sides and only the southerly direction is open to Bohai Bay. The combined effects of topography and weather produce relatively weak atmospheric pressure in Beijing throughout the year and a channel of cold sinking mountain air mixes with a piedmont wind belt to form a constraining field. This limiting effect on pollution dispersal in the urban area is no doubt harmful to human health (see also Xu 2007).

The elevated concentration of heavy metals especially Pb and Zn in the street dust can be attributed to vehicle emissions, abrasion or corrosion of the vehicle engine and body work (Fig. 12, Hoffmann *et al.* 1999; Matzka & Maher 1999; Goddu *et al.* 2004). Heavy vehicles and automobile emissions are predominant in samples from road sites and fossil fuel combustion can also contribute to the samples in winter.

#### 4.2 Traffic influences on magnetic properties

Magnetic compositions in street dust decreased significantly during Olympic Games (Figs 3 and 4) showing that magnetic measurement can serve as an efficient complementary tool for monitoring the effect of control measures. To improve air quality and create a pleasant environment for athletes, the Beijing Municipal Government enacted control regulations comprising closure/relocation of polluting industrial plants around Beijing accompanied by traffic control measures operating from 2008 July 1 to 2008 September 20. Trucks could only operate inside the 6th Ring Road from midnight to 6 a.m. and 300 000 'heavily emitting vehicles' were banned from roads through the city (Zhou *et al.* 2010). More rigid restrictions enforced after July 20th restricted private vehicle use and 70 per cent of government vehicles were ordered off the road thus reducing traffic by  $\sim 1.9$  million vehicles, or close to 60 per cent of the regular vehicular population (Wang *et al.* 2009 and references therein). As a result of aggressive traffic intervention, the road around the Olympic Park had become relatively less polluted by 2008 July but once traffic controls were withdrawn the road quickly became polluted again. This is demonstrated in the contour plots of magnetic susceptibility although  $\chi$  values on the 5th Ring Road remained higher than at other sites (Figs 3f–h) because heavy emitting traffic was barred from the roads inside of this Ring Road. By September pollution levels had rapidly returned to pre-Olympic levels (Figs 3 and 4) because (although heavy-emitting vehicles were still barred) private cars and sightseeing buses were allowed into the Park to view the games. Around Beichen East Road a large open parking lot was largely filled by private cars and sightseeing buses during daytime and the higher levels of  $\chi$  in sites on this road (Fig. 3g) reflect higher levels of anthropogenic contamination from this source. The high  $\chi$  value at location BJ23 in September likely results from heavy passenger and vehicular traffic at a crossroad just hundreds of metres south of the Olympic Park (Fig. 3g).

In a recent paper we reported magnetic properties of atmospheric dusts from the Chaoyang district collected between 2008 June and 2009 March (Qiao *et al.* 2011). The temporal distribution of magnetic concentration parameters in these dusts showed a similar trend to the street dust of this study with  $\chi$  decreasing significantly during the Olympic Games (see figs 3c and 5 in Qiao *et al.* 2011).

The susceptibility and concentration of air pollutants increased in the post-Olympic period (Qiao *et al.* 2011). This concisely demonstrates the effect that human-perturbation in emissions has on city air quality.

#### 4.3 Magnetic proxies for the city environment

Magnetic characterization of roadside dust provides first-order constraints on pollution patterns in highly populated urban areas (e.g. Charlesworth & Lees 1999; Roberston *et al.* 2003; Shiton *et al.* 2005; Kim *et al.* 2007) and the present investigation extends the scope of these studies showing that the highest concentrations of  $\chi$  and SIRM correspond to heavy traffic impact (Figs 2a and b). At most sites  $\chi$  values show distinctive seasonal patterns with higher values during the dry and cold winter months compared with warm and rainy summer months but the higher magnetic concentrations correlating with abandonment of traffic control measures demonstrate the modulating effect of traffic. Heavy metals show a robust correlation with the magnetic parameters  $\chi$ , SIRM and ARM (Table 3) and confirm the anthropogenic nature of the magnetic carriers. Magnetic susceptibility,  $\chi$ , shows the strongest correlation with heavy metals and this parameter provides a rapid assessment of degrees of heavy metal pollution.

### 5 CONCLUSIONS

This study has delineated the spatial and temporal characteristics of pollution in a sector of central Beijing before, during and after a major international event. Traffic is the major source of anthropogenic magnetic particle-induced enhancement of magnetic compositions in street dust; however, domestic combustion processes (mainly coal burning) are found to contribute a significant magnetic signature in the urban environment during the winter. Due to aggressive traffic intervention and emission control measures implemented during the Olympic Games, magnetic compositions in street dust decrease significantly. Significant correlations between  $\chi$  and heavy metals confirm that magnetic parameters are efficient environmental proxies of heavy metal pollution. Our results demonstrate that detailed measurements of magnetic properties on street dust in conjunction with geochemical analyses and electron microscope analyses can serve as an efficient complementary tool for monitoring problems related to urban environmental pollution.

#### ACKNOWLEDGMENTS

The authors thank the editor Cor Langereis and the two reviewers Mark J. Dekkers and Eduard Petrovský for constructive comments, which have greatly improved the manuscript. This work was financially supported by the National Nature Science Foundation of China (Grants 20677059, 40525013, 40804014 and 40821091).

#### REFERENCES

- Adachi, K. & Tainosho, Y., 2005. Single particle characterization of size-fractionated road sediments, *Appl. Geochem.*, **20**, 849–859.
- Adgate, J.L., Willis, R.D., Buckley, T.J., Chow, J.C., Weston, J.G., Rhoads, G.G. & Liou, P.J., 1998. Chemical mass balance source apportionment of lead in house dust, *Environ. Sci. Technol.*, **32**, 108–114.
- Almeida, S.M., Pio, C.A., Freitas, M.C., Reis, M.A. & Trancoso, M.A., 2006. Source apportionment of atmospheric urban aerosol based on weekdays/weekend variability: evaluation of road re-suspended dust contribution, *Atmos. Environ.*, **40**, 2058–2067.

- Angulo, E., 1996. The Tomlinson pollution load index applied to heavy metal 'Mussel-Watch' data: a useful index to assess coastal pollution, *Sci. Total Environ.*, **187**, 19–56.
- Banerjee, A.D.K., 2003. Heavy metal levels and solid phase speciation in street dusts of Delhi, India, *Environ. Pollut.*, **123**, 95–105.
- Beckwith, P.R., Ellis, J.B., Revitt, D.M. & Oldfield, F., 1986. Heavy metal and magnetic relationships for urban source sediments, *Phys. Earth planet. Inter.*, **42**, 67–75.
- Chaparro, M., Marié, D., Gogorza, C., Navas, A. & Sinito, A., 2010. Magnetic studies and scanning electron microscopy-X-ray energy dispersive spectroscopy analyses of road sediments, soils and vehicle-derived emissions, *Stud. Geophys. Geod.*, **54**, 633–650.
- Charlesworth, S.M. & Lees, J.A., 1997. The use of mineral magnetic measurements in polluted urban lakes and deposited dusts, Coventry, U.K., *Phys. Chem. Earth*, **22**, 203–206.
- Charlesworth, S.M. & Lees, J.A., 1999. Particulate associated heavy metals in the urban environment: their transport from source to deposit, Coventry, UK, *Chemosphere*, **39**, 833–848.
- Dearing, J.A., Hay, K.L., Baban, S.M.J., Huddleston, A.S., Wellington, E.M.H. & Loveland, P.J., 1996. Magnetic susceptibility of soil: an evaluation of conflicting theories using a national data set, *Geophys. J. Int.*, **127**, 728–734.
- Dekkers, M.J., 1997. Environmental magnetism: an introduction, *Geologie en Mijnbouw*, **76**, 163–182.
- Dekkers, M.J. & Pietersen, H.S., 1992. Magnetic properties of low-Ca fly ash: a rapid tool for Fe-assessment and a proxy for environmental hazard, in *Advanced Cementitious Systems: Mechanisms and Properties*, Vol. 245 pp. 37–47, ed. Glasser, F.P., McCarthy, G.J., Young, J.F., Masson, T.O. & Pratt, P.L., Mat. Res. Soc. Symposium Proceedings.
- Deng, C.L., Zhu, R.X., Verosub, K.L., Singer, M.J. & Vidic, N.J., 2004. Mineral magnetic properties of loess/paleosols couplets of the central loess plateau of China over the last 1.2 Myr, *J. geophys. Res. (B)*, **109**, doi:10.1029/2003JB002532.
- Dunlop, D.J., 2002. Theory and application of the Day plot (Mrs/Ms versus Bcr/Bc)1. Theoretical curves and tests using titanomagnetite data, *J. geophys. Res. (B)*, **107**, doi:10.1029/2001JB000486.
- Dunlop, D.J. & Özdemir, Ö., 1997. *Rock Magnetism: Fundamentals and Frontiers*, Cambridge University Press, UK.
- Evans, M.E., & Heller, F., 2003. *Environmental Magnetism: Principles and Applications of Enviromagnetics*, Academic Press, Oxford, UK.
- Feng, J.L., Chan, C.K., Fang, M., Hu, M., He, L.Y. & Tang, X.Y., 2005. Impact of meteorological and energy structure on solvent extractable organic compounds of PM2.5 in Beijing, China, *Chemosphere*, **61**, 623–632.
- Fergusson, J.E. & Kim, N., 1991. Trace elements in street and house dusts: source and speciation, *Sci. Total Environ.*, **100**, 125–150.
- Fialova, H., Maier, G., Petrovsky, E., Kapicka, A., Boyko, T., Scholger, R. & MAGPROX Team, 2006. Magnetic properties of soils from sites with different geological and environmental settings, *J. Appl. Phys.*, **59**, 273–283.
- Flanders, P.J., 1994. Collection, measurement, and analysis of airborne magnetic particulates from pollution in the environment, *J. Appl. Phys.*, **75**, 5931–5936.
- Frantzeskakis, J.M. & Frantzeskakis, M.J., 2006. Athens 2004 Olympic Games: transportation planning, simulation and traffic management, *ITE J.*, **76**, 26–32.
- Friedman, M.S., Powell, K.E., Hutwagner, L., Graham, L.M. & Teague, W.G., 2001. Impact of changes in transportation and commuting behaviors during the 1996 Summer Olympic Games in Atlanta on air quality and childhood asthma, *JAMA*, **285**, 897–905.
- Gautam, P., Blaha, U. & Appel, E., 2005. Magnetic susceptibility of dust-loaded leaves as a proxy of traffic-related heavy metal pollution in Kathmandu city, Nepal, *Atmos. Environ.*, **39**, 2201–2211.
- Goddu, S.R., Appel, E., Jordanova, D. & Wehland, F., 2004. Magnetic properties of road dust from Visakhapatnam (India)-relationship to industrial pollution and road traffic, *Phys. Chem. Earth*, **29**, 985–995.
- Hanesch, M., Scholger, R. & Rey, D., 2003. Mapping dust distribution around an industrial site by measuring magnetic parameters of tree leaves, *Atmos. Environ.*, **37**, 5125–5133.
- Harrison, R.M. & Yin, J.X., 2000. Particulate matter in the atmosphere: which particle properties are important for its effects on health? *Sci. Total Environ.*, **249**, 85–101.
- Heslop, H., 2009. On the statistical analysis of the rock magnetic S-ratio, *Geophys. J. Int.*, **178**, 159–161.
- Hoffmann, V., Knab, M. & Appel, E., 1999. Magnetic susceptibility mapping of roadside pollution, *J. Geochem. Explor.*, **66**, 313–326.
- Hopke, P.K., Lamb, R.E. & Natusch, D.F.S., 1980. Multi-elemental characterization of urban roadway dust, *Environ. Sci. Technol.*, **14**, 159–172.
- Hu, S.Y., Duan, X.M., Shen, M.J., Blaha, U., Roesler, W., Yan, H.T., Appel, E. & Hoffmann, V., 2008. Magnetic response to atmospheric heavy metal pollution recorded by dust-loaded leaves, *Chin. Sci. Bull. (in Chinese with English abstract)*, **53**, 1555–1564.
- Hunt, A., Jones, J. & Oldfield, F., 1984. Magnetic measurements and heavy metals in atmospheric particulates of anthropogenic origin, *Sci. Total Environ.*, **33**, 129–139.
- Jordanova, D., Hoffmann, V. & Febr, K.T., 2004. Mineral magnetic characterization of anthropogenic magnetic phases in the Danube river sediments (Bulgarian part), *Earth planet. Sci. Lett.*, **30**, 71–89.
- Kapicka, A., Petrovský, E., Ustjak, S. & Macháčková, K., 1999. Proxy mapping of fly-ash pollution of soils under a coal-burning power plant: a case study in the Czech Republic, *J. Geochem. Explor.*, **66**, 291–297.
- Kim, W., Doh, S.J., Park, Y.H. & Yun, S.T., 2007. Two-year magnetic monitoring in conjunction with geochemical and electron microscopic data of roadside dust in Seoul, Korea, *Atmos. Environ.*, **41**, 7627–7641.
- Kim, W., Doh, S.J., Yu, Y. & Lee, M., 2008. Role of Chinese wind-blown dust in enhancing environmental pollution in Metropolitan Seoul, *Environ. Pollut.*, **153**, 333–341.
- Kim, W., Doh, S.J., Yu, Y., 2009. Anthropogenic contribution of magnetic particulates in urban roadside dust, *Atmos. Environ.*, **43**, 3137–3144.
- King, J., Banerjee, S.K., Marvin, J. & Özdemir, Ö., 1982. A comparison of different magnetic methods for determining the relative grain size of magnetite in natural materials: some results from lake sediments, *Earth planet. Sci. Lett.*, **59**, 404–419.
- Knab, M., Appel, E. & Hoffmann, V., 2001. Separation of the anthropogenic portion of heavy metal contents along a highway by means of magnetic susceptibility and fuzzy C-means cluster analysis, *Eur. J. Environ. Eng. Geophys.*, **6**, 125–140.
- Lee, B.K., Jun, N.Y. & Lee, H.K., 2005. Analysis of impacts of urban air quality by restricting the operation of passenger vehicles during Asian Game events in Busan, Korea, *Atmos. Environ.*, **39**, 2323–2338.
- Li, P., Qiang, X.K., Xu, X.W., Li, X.B. & Sun, Y.F., 2010a. Magnetic properties of street dust: a case in Xi'an city, Shanxi province, China, *Chin. J. Geophys. (in Chinese with English abstract)*, **53**(1), 156–163.
- Li, Y., Shao, M., Lu, S.H., Chang, C.C. & Dasgupta, P.K., 2010b. Variations and sources of ambient formaldehyde for the 2008 Beijing Olympic games, *Atmos. Environ.*, **44**, 2632–2639.
- Liu, Q.S., Deng, C.L., Yu, Y. J., Torrent, J., Banerjee, S.K. & Zhu, R.X., 2005. Temperature dependence of magnetic susceptibility in an argon environment: implications for pedogenesis of Chinese loess/paleosols, *Geophys. J. Int.*, **161**, 102–112.
- Maher, B.A., 1988. Magnetic properties of some synthetic submicron magnetites, *Geophys. J. Roy. astr. Soc.*, **94**, 83–96.
- Maher, B.A., 1998. Magnetic properties of modern soils and Quaternary loessic paleosols: paleoclimatic implications, *Palaeogeogr. Palaeoclimatol. Palaeoecol.*, **137**, 25–54.
- Maher, B.A. & Thompson, R., 1999. *Quaternary Climates, Environments and Magnetism*, Cambridge University Press, Cambridge.
- Maher, B.A., Moore, C. & Matzka, J., 2008. Spatial variation in vehicle-derived metal pollution identified by magnetic and elemental analysis of roadside tree leaves, *Atmos. Environ.*, **42**, 364–373.
- Matzka, J. & Maher, B.A., 1999. Magnetic biomonitoring of roadside tree leaves: identification of spatial and temporal variations in vehicle-derived particulates, *Atmos. Environ.*, **33**, 4565–4569.
- Moreno, E., Sagnotti, L., Dinarè-Turell, J., Winkler, A. & Cascella, A., 2003. Biomonitoring of traffic air pollution in Rome using magnetic properties of tree leaves, *Atmos. Environ.*, **37**, 2969–2977.

- Morris, W.A., Versteeg, J.K., Bryant, D.W., Legzdins, A.E., McCarry, B.E. & Marvin, C.H., 1995. Preliminary comparisons between mutagenicity and magnetic susceptibility of respirable airborne particulate, *Atmos. Environ.*, **29**, 3441–3450.
- Muxworthy, A.R., Matzka, J. & Petersen, N., 2001. Comparison of magnetic parameters of urban atmospheric particulate matter with pollution and meteorological data, *Atmos. Environ.*, **35**, 4379–4386.
- Muxworthy, A.R., Schmidbauer, E. & Petersen, N., 2002. Magnetic properties and Mössbauer spectra of urban atmospheric particulate matter: a case study from Munich, Germany, *Geophys. J. Int.*, **150**, 558–570.
- Ng, S.L., Chan, L.S., Lam, K.C. & Chan, W.K., 2003. Heavy metal contents and magnetic properties of playground dust in Hong Kong, *Environ. Monit. Assess.*, **89**, 221–232.
- Oldfield, F., 1991. Environmental magnetism-A personal perspective, *Quat. Sci. Rev.*, **10**, 73–85.
- Olson, K.W. & Skogerboe, R.K., 1975. Identification of soil lead compounds from automotive sources, *Environ. Sci. Technol.*, **9**, 227–230.
- Omar, N.Y.M.J., Abas, M.R.B., Rahman, N.A., Tahir, N.M., Rushdi, A.I. & Simoneit, R.T., 2007. Levels and distributions of organic source tracers in air and roadside dust particles of Kuala Lumpur, Malaysia, *Environ. Geol.*, **52**, 1485–1500.
- Petrovský, E. & Ellwood, B.B., 1999. Magnetic monitoring of air-, land-, and water-pollution, in *Quaternary Climates, Environments and Magnetism*, eds Maher, B.A. & Thompson, R., Cambridge University Press, Cambridge, UK.
- Petrovský, E. & Kapička, A., 2006. On determination of the Curie point from thermomagnetic curves, *J. geophys. Res. (B)*, **111**, doi:10.1029/2006JB004507.
- Petrovský, E., Kapička, A., Zapletal, K., Šebestová, E., Spanilá, T., Dekkers, M.J., & Rochette, P., 1998. Correlation between magnetic parameters and chemical composition of lake sediments from Northern Bohemia-preliminary study, *Phys. Chem. Earth*, **23**, 1123–1126.
- Qiao, Q.Q., Zhang, C.X., Li, J., Li, H. & Huang, B.C., 2011. Magnetic properties and indicator of concentration of pollution of atmospheric dust in Chaoyang, Beijing, *Chin. J. Geophys. (in Chinese)*, **54**, 151–162.
- Roberston, D.J., Taylor, K.G. & Hoon, S.R., 2003. Geochemical and mineral magnetic characterization of urban sediment particulates, Manchester, UK, *Appl. Geochem.*, **18**, 269–282.
- Rogge, W.F., Mazurek, M.A., Hildemann, L.M., Cass, G.R. & Simoneit, B.R.T., 1993a. Quantification of urban organic aerosols at a molecular level: identification, abundance and seasonal variation, *Atmos. Environ.*, **27**, 1309–1330.
- Rogge, W.F., Hildemann, L.M., Mazurek, M.A., Cass, G.R. & Simoneit, B.R.T., 1993b. Sources of fine organic aerosol. 3. Road dust, tire debris, and organometallic brake lining dust: roads as sources and sinks, *Environ. Sci. Technol.*, **27**, 1892–1904.
- Sartor, J.D. & Gaboury, D.R., 1984. Street sweeping as a water pollution control measure: lessons learned over the past ten years, *Sci. Total Environ.*, **33**, 171–183.
- Shiton, V.F., Booth, C.A., Smith, J.P., Giess, P., Mitchell, D.J. & Williams, C.D., 2005. Magnetic properties of urban street dust and their relationship with organic matter content in the West Midlands, UK, *Atmos. Environ.*, **39**, 3651–3659.
- Spassov, S., Egli, R., Heller, F., Nourgaliev, D.K. & Hannam, J., 2004. Magnetic quantification of urban pollution sources in atmospheric particulate matter, *Geophys. J. Int.*, **159**, 555–564.
- Tanner, P.A., Ma, H.L. & Yu, P.K.N., 2008. Fingerprinting metals in urban street dusts of Beijing, Shanghai, and Hong Kong, *Environ. Sci. Technol.*, **42**, 7111–7117.
- Thompson, R. & Oldfield, F., 1986. *Environmental Magnetism*, Allen & Unwin, London.
- Tomilson, D.C., Wilson, J.G., Harris, C.R. & Jeffrey, D.W., 1980. Problems in assessment of heavy metals in estuaries and the formation of a pollution index, *Helgol. Meeresunters.*, **33**, 566–575.
- Utsunomiya, S. & Ewing, R.C., 2003. Application of high-angle annular dark field scanning transmission electron microscopy, scanning transmission electron microscopy energy-dispersive X-ray spectrometry, and energy-filtered transmission electron microscopy to the characterization of nanoparticles in the environment, *Environ. Sci. Technol.*, **37**, 786–791.
- Verosub, K.L. & Roberts, A.P., 1995. Environmental magnetism: past, present, and future, *Geophys. Res.*, **100**, 2175–2192.
- Wang, X., Westerdahl, D., Chen, L.C., Wu, Y., Hao, J.M., Pan, X.C., Guo, X.B. & Zhang, K.M., 2009. Evaluating the air quality impacts of the 2008 Beijing Olympic Games: on-road emission factors and black carbon profiles, *Atmos. Environ.*, **43**, 4535–4543.
- Weber, S., Hoffmann, P., Enslin, J., Dedik, A.N., Weinbruch, S., Miede, G., Gütlich, P. & Ortner, H.M., 2000. Characterization of iron compounds from urban and rural aerosol sources, *J. Aerosol. Sci.*, **31**, 987–997.
- Wise E.K. & Comrie A.C., 2005. Meteorologically adjusted urban air quality trends in the Southwestern United States, *Atmos. Environ.*, **39**, 2969–2980.
- Xie, S.J., Dearing, J.D., Bloemendal, J. & Boyle, J.F., 1999. Association between the organic matter content and magnetic properties in street dust, Liverpool, UK, *Sci. Total Environ.*, **241**, 205–214.
- Xie, S.J., Dearing, J.D. & Bloemendal, J., 2000. The organic matter content of street dust, Liverpool, UK and its association with dust magnetic properties, *Atmos. Environ.*, **34**, 269–275.
- Xie, S.J., Dearing, J.D., Boyle, J.F., Bloemendal, J. & Morse, A.P., 2001. Association between magnetic properties and element concentrations of Liverpool street dust and its implications, *J. appl. Geophys.*, **48**, 83–92.
- Yang, T., Liu, Q.S., Li, H.X., Zeng, Q.L. & Chan, L.S., 2010a. Anthropogenic magnetic particles and heavy metals in the road dust: magnetic identification and its implications, *Atmos. Environ.*, **44**, 1175–1185.
- Yang, T., Wang, Z.F., Zhang, B., Wang, X.Q., Wang, W., Gbauridi, A., & Gong, Y.B., 2010b. Evaluation of the effect of air pollution control during the Beijing 2008 Olympic Games using Lidar data, *Chin. Sci. Bull.*, **55**, 1311–1316.
- Yu, L.Z., Xu, Y. & Zhang, W.G., 1995. Magnetic measurement on lake sediment and its environmental application, *Prog. Geophys.*, **10**, 11–22.
- Zhang, C.X., Huang, B.C. & Li, Z.Y., 2006. Magnetic properties of highroad-side pine tree leaves in Beijing and their environmental significance, *Chin. Sci. Bull.*, **51**, 3041–3052.
- Zhang, C.X., Huang, B.C., Piper, J.D.A. & Luo, R.S., 2008. Biomonitoring of atmospheric particulate matter using magnetic properties of *Salix matsudana* tree ring cores, *Sci. Total Environ.*, **393**, 177–190.
- Zhang, C.X., Huang, B.C. & Liu, Q.S., 2009. Magnetic properties of different receptors around steel plants and their environmental significance, *Chin. J. Geophys. (in Chinese with English abstract)*, **52**, 2826–2839.
- Zhang, C.X., Liu, Q.S., Huang, B.C. & Su, Y.L., 2010. Magnetic enhancement upon heating of environmentally polluted samples containing haematite and iron, *Geophys. J. Int.*, **181**, 1381–1394.
- Zheng, Y. & Zhang, S.H., 2008. Magnetic properties of street dust and topsoil in Beijing and its environmental implications, *Chin. Sci. Bull.*, **53**, 408–417.
- Zhou, Y. et al., 2010. The impact of transportation control measures on emission reductions during the 2008 Olympic Games in Beijing, China, *Atmos. Environ.*, **44**, 285–293.